Hydrogen Peroxide Decomposition by Pyrite in the Presence of Fe(III)-ligands

P. Chiriță
Department of Inorganic, Analytical and Technological Chemistry,
University of Craiova, Calea Bucureşti 107I, Craiova 200478, Romania

Original scientific paper
Received: August 23, 2008
Accepted: February 24, 2009

The decomposition of hydrogen peroxide (H_2O_2) by pyrite in the presence of Fe(III)-ligands (sulfosalicylate (SSAL), ethylenediaminetetraacetate (EDTA), and phosphate) has been investigated in aqueous acidic media (pH 1) at 25 °C. It was found that H_2O_2 decomposition by pyrite was inhibited by the presence of EDTA, SSAL and phosphate. On the other hand, pyrite oxidation by H_2O_2 does not seem to be affected by the presence of Fe(III)-ligands. The experimental results demonstrate that H_2O_2 decomposition in the presence of Fe(III)-ligands is catalyzed by pyrite surface (a heterogeneous process). This process is first order with respect to $[H_2O_2]$. It is expected that the rate-determining step of the reaction mechanism of H_2O_2 decomposition in the presence of Fe(III)-ligands is one of the following two reactions:

$$\equiv FeHO_2^{2+} \rightarrow \equiv Fe^{2+} + HO_2^{\bullet}$$

$$\equiv Fe(OH)(HO_2)^{+} \rightarrow \equiv Fe^{2+} + HO_2^{\bullet} + HO^{-}$$

where ≡ denotes pyrite surface.

Key words:
Hydrogen peroxide, pyrite, Fe(III)-ligands, reaction mechanism

Introduction

The extraction of gold from pyrite matrix and desulphurization of coal are based on pyrite oxidation by an efficient reagent. The use of hydrogen peroxide (H_2O_2) as reagent for pyrite (FeS_2) oxidation is of particular interest.[1–4] H_2O_2 is a powerful oxidizing agent as depicted by the redox potential of 1.77 V.[5,6] The oxidation of FeS_2 by H_2O_2 in acidic media is characterized by the following overall reaction[1–4,7,8]

$$FeS_2 + 7.5\ H_2O_2 \rightarrow Fe^{3+}(aq) + 2\ SO_4^{2-}(aq) + H^+ + 7\ H_2O \quad (1)$$

The pyrite surface and the released ferric iron act as catalysts for H_2O_2 decomposition into H_2O and O_2 (stable products of H_2O_2 decomposition) causing a considerable loss of reagent[1–4,9]

$$H_2O_2 \rightarrow H_2O + 0.5\ O_2 \quad (2)$$

The H_2O_2 decomposition by pyrite surface (a heterogeneous process) is first order with respect to $[H_2O_2]$, and H_2O_2 decomposition by aqueous ferric iron (a homogeneous process) is first order with respect to both $[H_2O_2]$ and $[Fe^{3+}(aq)]$.[4] Taking into consideration the catalytic effect of aqueous ferric iron on H_2O_2 decomposition, it can be hypothesized that the process should be influenced by any complexing agent (Fe(III)-ligand) which is able to influence the catalytic activity of $Fe^{3+}(aq)$. Hence, the study of the H_2O_2 decomposition by pyrite in presence of Fe(III)-ligands may lead to the optimization of the hydrometallurgical process of pyrite oxidation by H_2O_2.

The objective of this study was to examine H_2O_2 decomposition by pyrite in acidic media in presence of Fe(III)-ligands, such as sulfosalicylate (SSAL), ethylenediaminetetraacetate (EDTA), and phosphate.

Experimental methods

Materials

All chemicals were of analytical grade and were used without further purification. Hydrochloric acid and hydrogen peroxide were used to obtain the desired pH and, respectively, oxidant concentration in each experiment. Doubly distilled water was used to prepare all solutions. Pyrite from Baia Mare region (Romania) was used for this study. Pyrite was characterized by wet chemical analysis and X-ray diffraction (XRD). The wet chemical analysis was performed using typical method.[10] Five elements (Co, Ni, Cu, Zn and As) were measured. XRD analysis was carried out on a CGR θ 60 diffractometer using CuKα monochromatic radiation (λ = 0.154 nm). The pyrite crystals were ground and classified into three size fractions by dry screening: 71–80 μm, 80–90 μm and 90–125 μm. The resulted fractions were treated for 1 min with nitric acid (c = 1 mol L^{-1}), washed repeatedly with doubly distilled water by rapid suspension, and de-

canted in order to remove fine particles. Then, each fraction was rinsed with fresh acetone several times and stored under oxygen-free desiccator. Only the 90−125 μm fraction was used for experiments. The specific surface area for this fraction, calculated for an assumed spherical geometry, is $s = 0.0112$ m^2 g^{-1}.[4]

Decomposition experiments and analytical determinations

H_2O_2 decomposition by pyrite was tested in the presence of three Fe(III)-ligands at initial pH 1, 25 °C temperature, $[H_2O_2]_o = 0.35$ mol L^{-1}, $s = 0.0112$ m^2 g^{-1} pyrite specific surface area, 250 mL of solutions, and $m = 0.3$ g pyrite. EDTA (ethylenediaminetetraacetic acid disodium salt:dihydrate, $Mr = 372.2$), SSA (sulfosalycilic acid, $Mr = 254.2$), and phosphate (sodium dihydrogen phosphate:monohydrate, $Mr = 138$) were used as Fe(III)-ligands. Their concentration ($c = 0.01$ mol L^{-1}) in the experiments was always higher than the concentration of total iron released during pyrite oxidation.

All decomposition experiments were carried out in a conventional gas meter placed in water batch controlled by a thermostat. In order to verify the tightness of gas meter it was necessary to run control experiments with pyrite and acidic solutions in the absence of H_2O_2. The volumes of released oxygen were corrected under laboratory conditions to find the corresponding decrease in hydrogen peroxide concentration (c_x/mol L^{-1}) as results of its decomposition into O_2 and H_2O (eq. 2).[4] To avoid an increase of H_2O_2 decomposition, no stirring system was used.

pH was monitored with an Ingold InLab 400 combined pH glass electrode incorporated in the gas meter. Before use, the electrode was calibrated in Mettler pH 4.01 and 7.00 buffers.

Duplicate experiments were carried out in order to study the pyrite oxidation by H_2O_2. Periodically, liquid samples were extracted from the gas meter with a syringe connected to a $d = 0.22$ μm filter. Liquid samples were analyzed for dissolved sulfate. The dissolved sulfate amounts were determined colourimetrically using the methylthymol blue method.[11] The oxidation degree of pyrite (α) was calculated by dividing the amount (mol) of released sulfate in the moment of sampling by the amount (mol) of sulfur contained in the pyrite at the beginning of experiments (i.e., 5 mmol S).

At the end of the experiments, the resulting solid residues were quickly rinsed with doubly distilled water, filtered throughout $d = 0.22$ μm membrane filter, dried and stored in an evacuated desiccator free of oxygen until analyzed by Fourier transform infrared spectroscopy (FTIR).

FTIR spectroscopy

FTIR spectroscopy was carried out using a Brucker ALPHA Fourier Transform Infrared Spectrometer, with a range of $\nu = 500-4000$ cm^{-1} and a resolution of 4 cm^{-1}; 28 scans were performed.

Results

Characterization of pyrite

X-ray diffraction analysis of the pyrite sample used in this study showed that it was cubic FeS_2. No other phases could be detected. The wet chemical analysis showed that pyrite sample had a composition close to the stoichiometric ratio expected for this mineral ($\nu_{S/Fe} = 1.98 \pm 0.03$). The mass fractions of the minor elements analyzed were: $w_{Co} = 0.02$ %; $w_{Ni} = 0.02$ %; $w_{Cu} = 0.01$ %; $w_{Zn} = 0.01$ % and $w_{As} = 0.13$ %. Fig. 1 shows FTIR spectrum of pyrite sample after grinding (unclean sample), indicating presence of several oxidation products on mineral surface. There are various patterns in the $\nu = 500-1626$ cm^{-1} region. The broad band around $\nu = 3233$ cm^{-1} includes peaks from water, ferric hydroxide and/or ferric oxy-hydroxide.[12,13] The 500−1200 cm^{-1} region shows that the unclean pyrite sample consists of products of sulfur oxidation (the signals at 1109, 1069, 1011, 665 and 602 cm^{-1} that may be assigned to sulfate, sulfite and thiosulfate[12,13]) and, respectively, iron oxidation (the peaks at 811 and 523 cm^{-1} that may be attributed to amorphous or poorly crystalline ferric hydroxides and oxides[12,13]). The peak at 1454 cm^{-1} can be assigned to carbonate ions.[14] FTIR spectrum of pyrite sample prepared by the previously described cleaning procedure (clean sample) is also shown in Fig. 1. No oxidation compounds were observed in this pyrite sample.

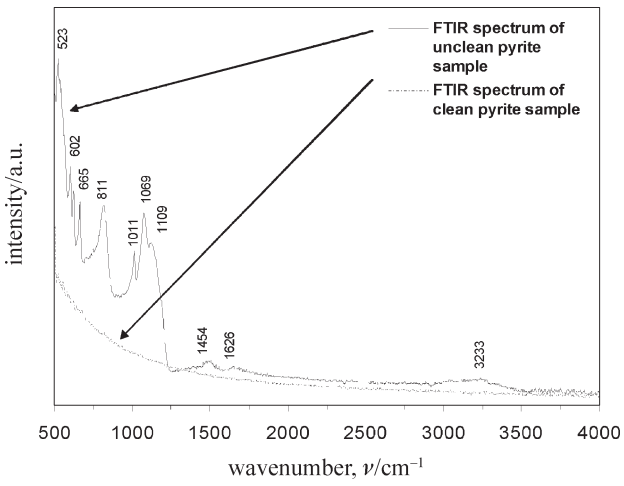

Fig. 1 – *FTIR spectra for unclean and clean pyrite sample*

H_2O_2 decomposition by pyrite in the presence of Fe(III)-ligands

The results (c_x/mol L^{-1}) of the experiments performed in the presence of SSAL, EDTA and phosphate ($c = 0.01$ mol L^{-1}) and in the absence of Fe(III)-ligands are shown in Fig. 2. At 25 °C, pH 1, and in the presence of Fe(III)-ligands, the c_x vs. t curves indicate a parabolic trend. In the absence of Fe(III)-ligands the c_x vs. t curve indicates an exponential trend. Therefore, after a decomposition period of 180 min, in the absence of Fe(III)-ligands, c_x was higher than that measured in the presence of SSAL, EDTA or phosphate. These results indicate that H_2O_2 decomposition by pyrite is inhibited by the presence of EDTA, SSAL, and phosphate (Fe(III)-ligands). The c_x values registered in the course of experiments conducted in the presence of EDTA and SSAL were higher than those registered in the course of experiments carried out in the presence of phosphate. This could be the result of a possible ligand concentration decrease due to the EDTA and SSAL (organic compounds) oxidation by H_2O_2/Fe system (Fe from pyrite).[15] However, no attempts were made in order to quantify the concentration of EDTA and SSAL in the course of the experiments. We may note that during the H_2O_2 decomposition experiment conducted in the presence of SSAL the intensity of solution colour (red, due to Fe(SSAL)$^+$ complex[16]) gradually increased, suggesting that there was sufficient SSAL in the solution to react with the released ferric iron.

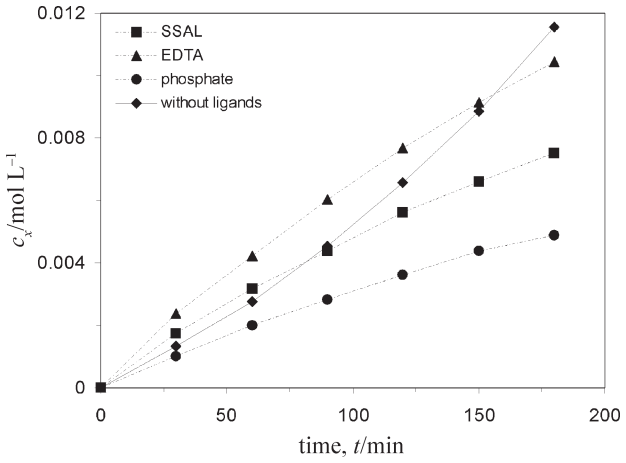

F i g . 2 – *Results of H_2O_2 decomposition by pyrite in acidic media (in the presence and absence of Fe(III)-ligands)*

Pyrite oxidation by H_2O_2 in the presence of Fe(III)-ligands

The oxidation degree of pyrite (α) in the presence of Fe(III)-ligands is shown in Fig. 3. Fig. 3 also shows the oxidation degree of pyrite registered during experiment without Fe(III)-ligands. As may

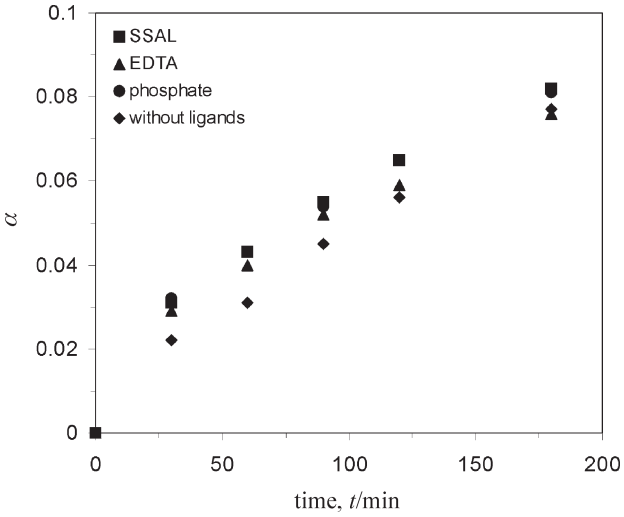

F i g . 3 – *Results of pyrite oxidation by H_2O_2 in acidic media (in the presence and absence of Fe(III)-ligands)*

be seen from this figure, the values of α, in the presence and absence of Fe(III)-ligands, are practically identical. The α values registered after 180 min of pyrite oxidation are: 0.077 (in absence of ligands), 0.076 (in presence of EDTA), 0.082 (in presence of SSAL) and 0.081 (in presence of phosphate). These observations suggest that the pyrite oxidation by H_2O_2 is not significantly influenced by the presence of Fe(III)-ligands.

The pH measurements carried out during the H_2O_2 decomposition experiments, in the presence and absence of Fe(III)-ligands, showed that the proton concentration (10^{-pH}) remained constant after $t = 180$ min of reaction. These results indicate that the protons production or consumption, during the experimental runs, is insignificant with respect to their initial concentration ($c_0 = 0.1$ mol L^{-1}).

FTIR analysis of reacted pyrite samples

In order to study the interaction between pyrite surface and Fe(III)-ligands, FTIR spectroscopy was used. The FTIR spectra of reacted samples are presented in Figs. 4a, 4b and 4c. FTIR spectra of EDTA, phosphate and clean pyrite sample are also given for comparison. No "testifier" spectrum was recorded for SSAL (an aqueous solution of $w = 30$ % SSAL was used for the preparation of experimental solutions). The main feature noted from the analysis of collected FTIR spectra is that the spectrum of clean pyrite and that of pyrite reacted in the presence of all Fe(III)-ligands were similar in the $\nu = 500$-4000 cm^{-1} region. This observation indicates that there are no notable interactions between Fe(III)-ligands and pyrite surface. This could be due either to the little number of adsorption centers for SSAL, EDTA and phosphate on pyrite surface or to the low affinity of Fe(III)-ligands for pyrite surface.

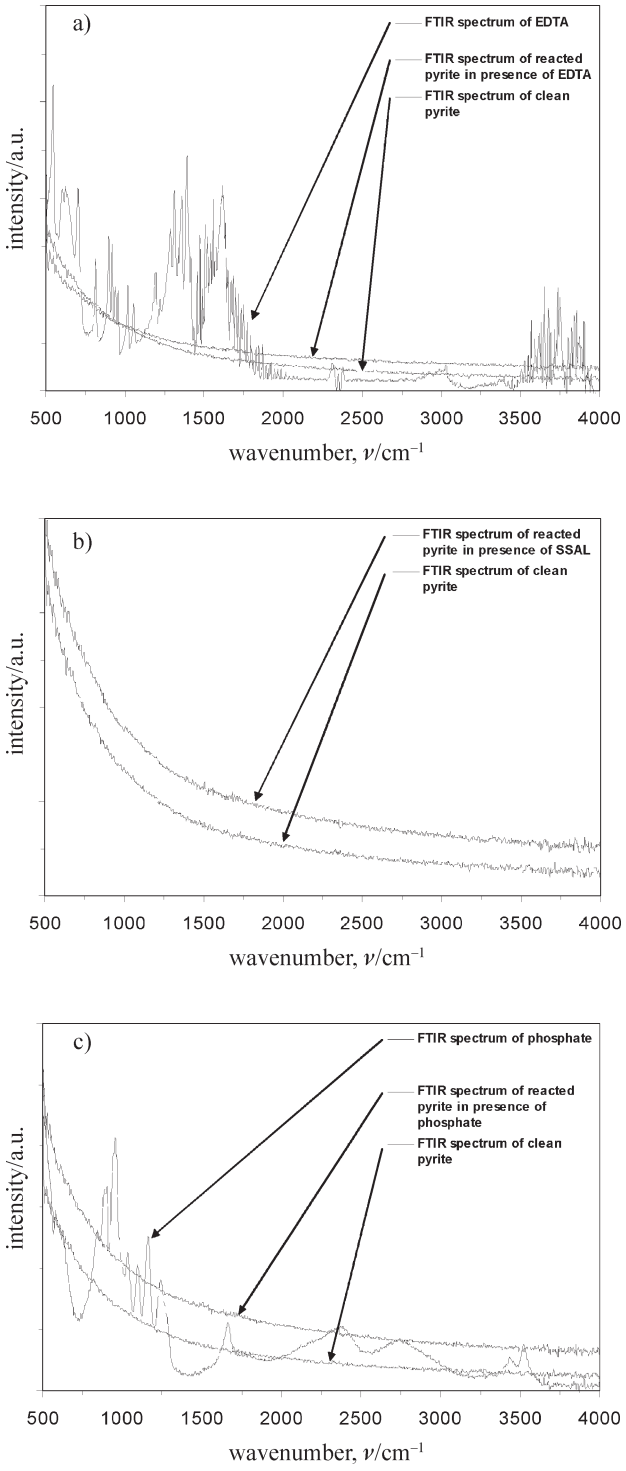

F i g . 4 – *FTIR spectra for clean pyrite sample and reacted pyrite samples in the presence of (a) EDTA, (b) SSAL and (c) phosphate. FTIR spectra of (a) EDTA and (c) phosphate are shown for comparison.*

Discussion

The experimental data presented above indicate that, on one hand, the H_2O_2 decomposition by pyrite is inhibited by the presence of SSAL, EDTA, and phosphate and, on the other hand, the presence of Fe(III)-ligands do not influence pyrite oxidation by H_2O_2. Also, it is important to note that FTIR analysis of reacted pyrite samples indicates that the adsorption degree of SSAL, EDTA and phosphate to pyrite surface is insignificant. All these results suggest an intricate interaction between pyrite and H_2O_2 in the presence of Fe(III)-ligands. In the next sections we will discuss the details of this interaction starting from the above-mentioned experimental data.

Rate-determining step of pyrite oxidation by H_2O_2

The data given in Fig. 3 were analyzed with the aid of the Shrinking core model controlled by chemical reaction at the unreacted particle surface[5,17]

$$1-(1-\alpha)^{1/3} = k_r t \qquad (3)$$

where: α is the fraction of oxidized pyrite, k_r is rate coefficient and t is time. Fig. 5 shows that the Shrinking core model controlled by chemical reaction at the unreacted particle surface represented by eq. (3) describes very well the experimental data obtained in this study. Correlation coefficients of above 0.99 were obtained in all of the cases. This finding indicates that a surface chemical reaction is the rate controlling step of pyrite oxidation by H_2O_2 both in the absence and presence of Fe(III)-ligands. Moreover, the obtained values of k_r (Table 1) are practically equal indicating that the pyrite oxidation by H_2O_2 is not influenced by the presence of Fe(III)-ligands after 180 min of reaction at 25 °C and pH 1.

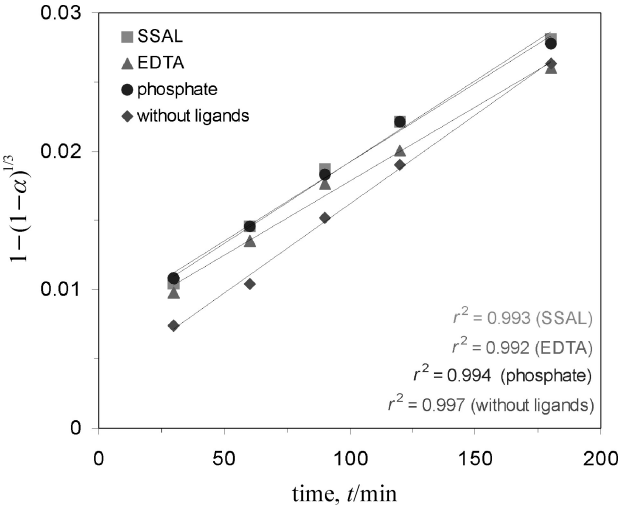

F i g . 5 – *Experimental data of pyrite oxidation by H_2O_2 in acidic media (in the presence and absence of Fe(III)-ligands) plotted according to eq. (5) (Shrinking core model controlled by chemical reaction at the unreacted particle surface).*

Kinetics of H_2O_2 decomposition by pyrite in the presence of Fe(III)-ligands

Chirita[4] found that the data obtained in the experiments of H_2O_2 decomposition by pyrite in acidic media (in the absence of Fe(III)-ligands) can be fitted by following equation

$$\ln R = k_a(1 + N \cdot [H_2O_2]_0)\, t \qquad (4)$$

where $R = \dfrac{(1 + N \cdot c_x) \cdot [H_2O_2]_0}{[H_2O_2]_0 - c_x}$, $N = \dfrac{k_b}{k_a}$, k_a (min^{-1}) and k_b (L mol^{-1} min^{-1}) are the rate coefficients of heterogeneous and, respectively, homogeneous H_2O_2 decomposition by pyrite in acidic media, $[H_2O_2]_0$ is the initial concentration of H_2O_2, and c_x (mol L^{-1}) is the decrease in H_2O_2 concentration as results of its decomposition into O_2 and H_2O. Indeed, eq. (4) fits very well the experimental data obtained in the absence of Fe(III)-ligands (Fig. 6a). The coefficient of correlation was $r^2 = 0.997$ for $N = 45$. The rate coefficients are shown in Table 1. Unfortunately, eq. (4) gave a poor fit to experimental data obtained in experiments conducted in the presence of Fe(III)-ligands (for different N within range $10^{-5}-10^5$). Instead, the following equation (first order kinetics equation)[4]

$$\ln \frac{[H_2O_2]_0}{[H_2O_2]_0 - c_x} = kt \qquad (5)$$

where k is the rate coefficient, fits well with the experimental data obtained in experiments with Fe(III)-ligands (Fig. 6b). The coefficients of correlation (r^2) were higher than 0.98. The rate coefficients are listed in Table 1. These findings could be explained starting from the proposed model for H_2O_2 decomposition by pyrite in acidic media.[4] According to this model the H_2O_2 decomposition by pyrite (pH from 1 to 2 and temperatures from 25 to 45 °C) is double catalyzed by pyrite surface (a heterogeneous process) and Fe^{3+}(aq) (a homogeneous process). Assuming that the homogeneous reaction is suppressed by the complexation of Fe^{3+}(aq) with SSAL, EDTA and phosphate, it results that, in the presence of Fe(III)-ligands, H_2O_2 decomposition by pyrite is catalyzed only by pyrite surface (heterogeneous reaction). There are three main experimental findings that suggest this assumption. First, the parabolic trends of H_2O_2 decomposition curves registered in presence of SSAL, EDTA and phosphate vs. the exponential trend registered in the

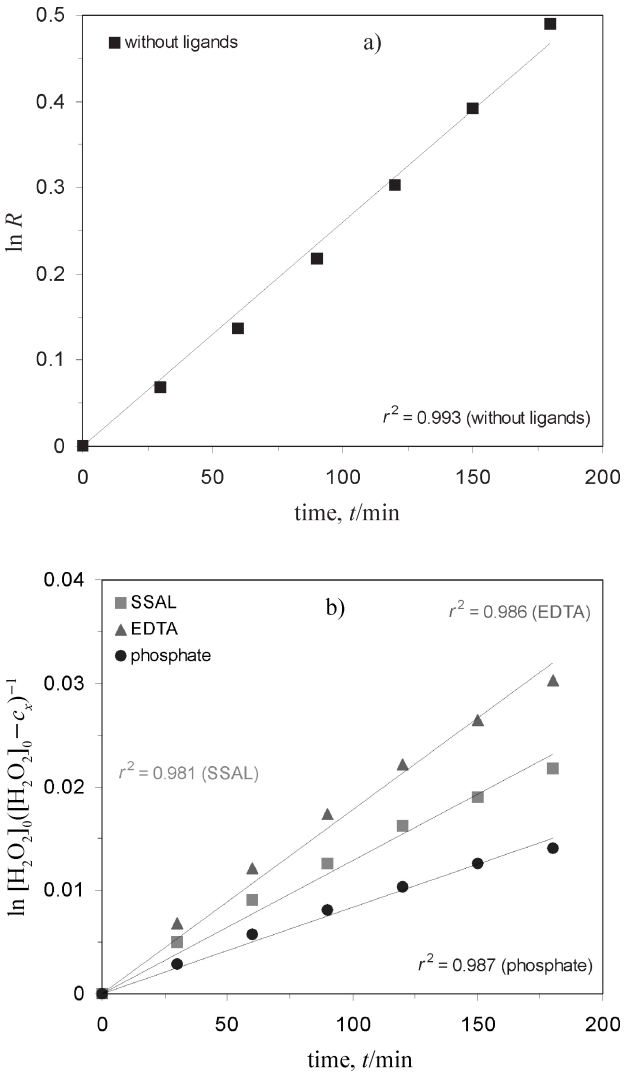

Fig. 6 – *(a) Experimental data of H_2O_2 decomposition by pyrite in the absence of Fe(III)-ligands plotted according to the kinetic model proposed by Chirita.[4] (b) Experimental data of H_2O_2 decomposition by pyrite in the presence of Fe(III)-ligands plotted according to eq. (5).*

Table 1 – *Summary of experimental results*

	SSAL	EDTA	Phosphate	Without ligands
k_r/min^{-1}	$1.2 \cdot 10^{-4}$ ($\pm 5.7 \cdot 10^{-6}$)	$1.1 \cdot 10^{-4}$ ($\pm 5.6 \cdot 10^{-6}$)	$1.1 \cdot 10^{-4}$ ($\pm 5.1 \cdot 10^{-6}$)	$1.3 \cdot 10^{-4}$ ($\pm 3.9 \cdot 10^{-6}$)
k_a/min^{-1}	–	–	–	$1.3 \cdot 10^{-4}$ ($\pm 4.5 \cdot 10^{-6}$)
k_b/L^{-1} mol^{-1} min^{-1}	–	–	–	$5.9 \cdot 10^{-3}$ ($\pm 1.78 \cdot 10^{-4}$)
$k(k_A)$/min^{-1}	$1.4 \cdot 10^{-4}$ ($\pm 3.8 \cdot 10^{-6}$)	$1.9 \cdot 10^{-4}$ ($\pm 4.5 \cdot 10^{-6}$)	$0.9 \cdot 10^{-4}$ ($\pm 1.7 \cdot 10^{-6}$)	–

absence of Fe(III)-ligands (Fig. 2). The different trends suggest different reaction pathways. Second, the FTIR spectra of residual pyrite samples (Fig. 4) suggesting an unchanged pyrite surface in the presence of Fe(III)-lignads. Third, the results obtained from the experiment designated to study the pyrite oxidation by H_2O_2 indicating a similar reactivity of pyrite surface both in the absence and presence of Fe(III)-ligands.

The heterogeneous H_2O_2 decomposition is a first order reaction with respect to $[H_2O_2]$:[4]

$$r = k_A [H_2O_2] \tag{6}$$

where r is the rate of H_2O_2 decomposition in presence of Fe(III)-ligands, k_A (min^{-1}) is the rate coefficient, and $[H_2O_2]$ is the hydrogen peroxide concentration.

Integrating eq. (7).

$$r = -\frac{d[H_2O_2]}{dt} = k_A [H_2O_2] \tag{7}$$

and rearranging the terms of obtained relation we get:

$$-\ln [H_2O_2] + C = k_A t \tag{8}$$

where C is a constant. From initial conditions $t_0 = 0$ and $[H_2O_2] = [H_2O_2]_0$ (for $t_0 = 0$) one obtains:

$$C = \ln [H_2O_2]_0 \tag{9}$$

Combining eq. (8) and eq. (9), taking into account that $[H_2O_2] = [H_2O_2]_0 - c_x$ and rearranging the terms one obtains:

$$\ln\left(\frac{[H_2O_2]_0}{[H_2O_2]_0 - c_x}\right) = k_A t \tag{10}$$

The similarity between the theoretical equation (eq. (10)) and eq. (5) (that fits the experimental data) demonstrates the consistency of measured rate coefficients with eq. (5) and supports the hypothesis that H_2O_2 decomposition by pyrite in the presence of Fe(III)-ligands is catalyzed only by pyrite surface. Note that the quasi-equality between the rate coefficients (average $k_A = 1.4 \cdot 10^{-4}$ min^{-1}) of H_2O_2 decomposition by pyrite in the presence of Fe(III)-ligands and the rate coefficient ($k_a = 1.3 \cdot 10^{-4}$ min^{-1}) corresponding to heterogeneous decomposition of H_2O_2 by pyrite in the absence of Fe(III)-ligands (Table 1) is also consistent with the basic assumption of the proposed model of H_2O_2 decomposition by pyrite in the presence of Fe(III)-ligands.

It is expected that the rate-determining step of the reaction mechanism of H_2O_2 decomposition in the presence of Fe(III)-ligands is one of the following two reactions

$$\equiv FeHO_2^{2+} \rightarrow \equiv Fe^{2+} + HO_2\cdot \tag{11}$$

$$\equiv Fe(OH)(HO_2)^{+} \rightarrow \equiv Fe^{2+} + HO_2\cdot + HO^{-} \tag{12}$$

where ≡ denotes pyrite surface. The rate-determining step, which supposes the decomposition of the surface complexes ($\equiv FeHO_2^{2+}$ or $\equiv Fe(OH)(HO_2)^{+}$) and regeneration of surface ferrous iron ($\equiv Fe^{2+}$), was established taking into consideration the results of previous studies concerning H_2O_2 decomposition by ferric iron[18–20] and by pyrite.[4]

Conclusions

The H_2O_2 decomposition by pyrite in acidic media (pH 1 at 25 °C) in the presence of Fe(III)-ligands ($c = 0.01$ mol L^{-1}) was studied. It was found that the reaction pathway of H_2O_2 decomposition by pyrite is affected by the addition of SSAL, EDTA and phosphate; H_2O_2 decomposition is inhibited by the presence of Fe(III)-ligands. However, pyrite oxidation by H_2O_2 does not seem to be influenced by the presence of Fe(III)-ligands, after $t = 180$ min of reaction.

Because the ligands are able to sequester the aqueous ferric iron, the H_2O_2 decomposition by pyrite in the presence of SSAL, EDTA and phosphate is catalyzed only by the pyrite surface (a first order reaction with respect to $[H_2O_2]$).

ACKNOWLEDGEMENTS

I thank three anonymous reviewers for their rigorous and valuable critique of the manuscript.

List of symbols

- c – concentration, mol L^{-1}
- c_x – extensive quantity for all concentration, mol L^{-1}
- k_a – rate coefficient for a first order reaction, min^{-1}
- k_r – rate coefficient for a first order reaction, min^{-1}
- $k(k_A)$ – rate coefficient for a first order reaction, min^{-1}
- k_b – rate coefficient for a second order reaction, L mol^{-1} min^{-1}
- Mr – molecular mass
- m – mass, g
- r^2 – correlation coefficient
- s – specific surface area, m^2 g^{-1}
- t – time, min
- w – mass percentage, %
- α – degree of dissolution
- ν – stoichiometric ratio
- ν – wavenumber, cm^{-1}

References

1. *Dimitrijevic, M., Antonijevic, M. M., Jankovic, Z.*, Hydrometallurgy **42** (1996) 377.
2. *Dimitrijevic, M., Antonijevic, M. M., Dimitrijevic, V.*, Miner. Eng. **12** (1999) 165.
3. *Antonijevic, M. M., Jankovic, Z. D., Dimitrijevic, M. D.*, Hydrometallurgy **71** (2004) 329.
4. *Chirita, P.*, Chem. Biochem. Eng. Q. **21** (3) (2007) 257.
5. *Adebayo, A. O., Ipinmoroti, K. O., Ajayi, O. O.*, Chem. Biochem. Eng. Q. **17** (3) (2003) 213.
6. *Moussavi, G., Naddafi, K., Mesdaghinia, A., Mohsenic, M.*, Chem. Biochem. Eng. Q. **22** (1) (2008) 9.
7. *Lefticariu, L., Schimmelmann, A., Pratt, L. M., Ripley, E. M.*, Geochim. Cosmochim. Acta **71** (2007) 5072.
8. *Lefticariu, L., Pratt, L. M., Ripley, E. M.*, Geochim. Cosmochim. Acta **70** (2006) 4889.
9. *Chirita, P., Descostes, M.*, J. Colloid Interface Sci. **299** (2006) 260.
10. *Jeffery, P. G.,* Chemical Methods of Rock Analysis (Second Edition). Pergamon Press, Oxford, 1975.
11. *Madsen, B. C., Murphy, R. J.*, Anal. Chem. **53** (1981) 1924.
12. *Mikhlin, Yu. L., Kuklinskiy, A. V., Pavlenko, N. I., Varnek, V. A., Asanov, I. P., Okotrub, A. V., Selyutin, G. E., Solovyev, L. A.*, Geochim. Cosmochim. Acta **66** (2003) 4057.
13. *Chirita, P., Descostes, M., Schlegel, M. L.*, J. Colloid Interface Sci. **321** (2008) 84.
14. *Descostes, M., Beaucaire, C., Mercier, F., Savoye, S., Sow, J., Zuddas, P.*, Bull. Soc. Geol. France **173** (2002) 265.
15. *Kwan, W. P., Voelker, B.*, Environ. Sci. Technol. **36** (2002) 1467.
16. *Liteanu, C., Hopirteanu, E.*, Chimie analitica cantitativa. Volumetria, Editura Didactica si Pedagogica, Bucuresti 1972.
17. *Ciminelli, V. S. T., Osseo-Asare, K.*, Metallurgical and Materials Transactions B **26(B)** (1995) 209.
18. *De Laat, J., Le, T. G.*, Appl. Catal. B: Environ. **66** (2006) 137.
19. *Glin, S. S., Gurol, M. D.*, Environ. Sci. Technol. **32** (1998) 1417.
20. *Shukla, R. S., Pant, R. P.*, J. Colloid Interface Sci. **268** (2003) 168.